Appl Microbiol Biotechnol (2015) 99:6059–6068
DOI 10.1007/s00253-015-6457-9

ENVIRONMENTAL BIOTECHNOLOGY

Biodegradation of fat, oil and grease (FOG) deposits under various redox conditions relevant to sewer environment

Xia He · Qian Zhang · Michael J. Cooney · Tao Yan

Received: 19 December 2014 / Revised: 30 January 2015 / Accepted: 1 February 2015 / Published online: 26 February 2015
© Springer-Verlag Berlin Heidelberg 2015

Abstract Fat, oil and, grease (FOG) deposits are one primary cause of sanitary sewer overflows (SSOs). While numerous studies have examined the formation of FOG deposits in sewer pipes, little is known about their biodegradation under sewer environments. In this study, FOG deposit biodegradation potential was determined by studying the biodegradation of calcium palmitate in laboratory under aerobic, nitrate-reducing, sulfate-reducing, and methanogenic conditions. Over 110 days of observation, calcium palmitate was biodegraded to CO_2 under aerobic and nitrate-reducing conditions. An approximate 13 times higher CO_2 production rate was observed under aerobic condition than under nitrate-reducing condition. Under sulfate-reducing condition, calcium palmitate was recalcitrant to biodegradation as evidenced by small reduction in sulfate. No evidence was found to support calcium palmitate degradation under methanogenic condition in the simulated sewer environment. Dominant microbial populations in the aerobic and nitrate-reducing microcosms were identified by Illumina seqeuncing, which may contain the capability to degrade calcium palmitate under both aerobic and nitrate-reducing conditions. Further study on these populations and their functional genes could shed more light on this microbial process and eventually help develop engineering solutions for SSOs control in the future.

Keywords Fat, oil and grease (FOG) deposits · Biodegradation · Redox conditions · Sewer systems

X. He · Q. Zhang · T. Yan (✉)
Department of Civil and Environmental Engineering, University of Hawaii at Manoa, Honolulu, HI 96822, USA
e-mail: taoyan@hawaii.edu

M. J. Cooney
Hawaii Natural Energy Institute, University of Hawaii at Manoa, Honolulu, USA

Introduction

Fat, oil and grease (FOG) deposits are hardened and insoluble solid formations that can significantly reduce and sometimes completely block the flow of wastewater in sewer lines. Among thousands of sanitary sewer overflows (SSOs) due to line blockages in the USA, 47 % are related to FOG deposits (USEPA 2004). FOG deposits are conventionally believed to be simply solidified FOG wastes poured down sinks and drains. However, a recent study showed that 16 out of 19 FOG deposit samples (84 %) contained more than 50 % lipid with the primary lipid being palmitic (Keener et al. 2008). Most of the FOG deposit samples (85 %) exhibited rigid sandstone-like texture with high yield strength, while chemical analyses identified calcium as the primary metal with the largest concentration of calcium being 19.8 % which suggests that FOG deposits are likely calcium salts of fatty acids (Keener et al. 2008). This hypothesis was supported by a subsequent study indicating that FOG deposits were formed as a result of saponification as well as the aggregation of excess calcium and unreacted free fatty acids (He et al. 2011). Long-chain fatty acids (LCFAs) between C14 and C18 make up the majority of FOG deposits, with palmitic acid (C16) being the most abundant (He et al. 2011; Keener et al. 2008; Williams et al. 2012).

This new understanding of the chemical composition of FOG deposits has spurred interests in both understanding the sources of calcium and LCFAs and the biodegradation of calcium salts of LCFAs in sewer systems. Municipal wastewater naturally contains certain levels of calcium, and concrete sewer pipes can also release calcium as a result of sewer crown corrosion (He et al. 2013; Pagaling et al. 2014). High levels of fatty acids can be introduced into sewer systems from various sources, such as food frying (Canakci 2007), household detergents (Lee et al. 2013), and food processing industry (Li et al. 2002). However, no study has been reported to investigate the biodegradation of calcium salts of LCFAs in FOG deposits

(e.g., calcium palmitate). This is important as the accumulation of FOG deposits in sewer lines is the net outcome of formation and biodegradation of FOG deposits.

Previous studies on the biodegradation of LCFAs were conducted under strict anaerobic conditions (mostly for anaerobic digesters), while few studies have investigated LCFA biodegradation under other redox conditions, which may be relevant to sewer systems. The biodegradation potential of LCFAs in anaerobic digesters was often very low, which was attributed to their inhibitory effects on microorganisms (Alves et al. 2009; Becker et al. 1999; Lalman and Bagley 2000, 2001; Li et al. 2005; Pereira et al. 2005; Salam et al. 2012; Shin et al. 2003). LCFAs are believed to adhere to outer surfaces of microbial cells, creating a physical barrier that disrupts various cellular functions (e.g., nutrient transport and waste excretion) (Alves et al. 2009; Pereira et al. 2005; Salam et al. 2012). However, some bacterial species working in synergistic mode, such as *Syntrophomonas* species and *Thermosyntrophalipolytica* of the family *Syntrophomonadaceae* (Alves et al. 2009; Hatamoto et al. 2007; Sousa et al. 2007), were capable of effectively degrading LCFAs. Furthermore, the addition of calcium enhanced the biodegradation of LCFAs in anaerobic digesters (Hatamoto et al. 2007; Roy et al. 1985), suggesting that calcium salts of LCFAs in FOG deposits may be biodegradable in sewer environments.

In this study, the biodegradation potential of the calcium salts of LCFAs in FOG deposits under various redox conditions relevant to sewer systems, including aerobic, nitrate-reducing, sulfate-reducing, and methanogenic conditions, was investigated in laboratory microcosms using calcium palmitate as the model compound. The biodegradation of calcium palmitate was examined by monitoring CO_2 generation, active biomass as total protein, reduction of electron acceptors such as nitrate and sulfate, and fatty acid profiles. Microbial community changes over time in the different redox conditions were also determined by Illumina sequencing of 16S ribosomal RNA (rRNA) gene amplicons. The changes of microbial community structure were compared so as to infer the microbes responsible for biodegradation and provide fundamental insights into biodegradation of FOG deposits in sewer environments.

Materials and methods

Microcosm setup

Laboratory microcosms were constructed in flasks for the aerobic condition (Fig. 1) or in serum bottles for anaerobic conditions. Calcium palmitate ($[CH_3(CH_2)_{14}COO]_2Ca$), as the model compound for FOG deposits, was used as the sole carbon source in the microcosm experiments. Microcosm setup for aerobic and anaerobic conditions was described separately in detail in the following paragraphs. Triplicate microcosms were set up for each redox condition. All microcosms were inoculated with microorganisms extracted from a real FOG deposit sample collected from a sewer pipe in the City of Honolulu. The FOG deposit sample (1 g) was grinded into small particles and then mixed with 20 ml PBS buffer (pH=7.4). Then 1 ml PBS buffer was centrifuged at 10,000×*g* for 5 min, and the precipitate was used as inoculum. Calcium (final concentration: 400 mg/l) was amended to all microcosms on day 80 and day 88.

The microcosms for aerobic condition contained 0.005 M calcium palmitate and 150 ml artificial wastewater in 250-ml flasks. The artificial wastewater contains per liter of deionzied water: NH_4Cl 0.2 g, KCl 0.33 g, $MgCl_2.6H_2O$ 0.1 g, 0.04 M potassium phosphate buffer (pH=7), NaCl 5 g (for aerobic, methanogenic conditions, and negative control) or $NaNO_3$ 5 g (for nitrate redox condition) or Na_2SO_4 5 g (for sulfate redox condition), yeast extract 0.006 g, and trace element 1 ml (He et al. 2005). Air was continuously pumped through the experimental systems to provide aeration as shown in Fig. 1. Air was first pumped into two sequential tanks containing 1 liter saturated $Ca(OH)_2$ (1.6 g/l) to remove CO_2 in the air. The purified air was then bubbled into five testing flasks, three for aerobic tests (with microbial inoculation) and two for CO_2 control (without microbial inoculation). CO_2 generated in the microcosms was subsequently captured by bubbling into a CO_2 collecting flask with 350 ml saturated $Ca(OH)_2$ solution. The $CaCO_3$ formed in the CO_2 collecting flasks was quantified to indicate the biodegradation of calcium palmitate. pH was monitored in all saturated $Ca(OH)_2$ solutions, and the solutions were replaced when the pH was below 9. Gas meters were used to maintain the incoming airflow at 0.5 ml/s in each testing flask. All five flasks were continuously stirred using a magnetic stirrer under room temperature (25 °C).

Anaerobic microcosms were established in 160-ml serum bottles under an atmosphere of 100 % N_2. All microcosms contained 0.005 M calcium palmitate in 100 ml artificial wastewater. The bottles were sealed with Teflon rubber stopers and aluminum crimps. The serum bottles for negative control (no microbial activity) were autoclaved at 120 °C for 20 min at day 0. At each sampling point, the microcosms were rigorously shaken and sampled with sterile syringes. To maintain anaerobic condition, the bottles were flushed with N_2 gas for 10 min after sampling. All bottles were shaken at 40 rpm and incubated in the dark at 25 °C. Both gas and liquid samples were collected from each microcosm once a week, and the samples were immediately analyzed.

Measurement of CO_2, CH_4, pH, nitrate and sulfate

Under aerobic condition, gas phase CO_2 was determined by measuring the precipitation of $CaCO_3$ in the CO_2

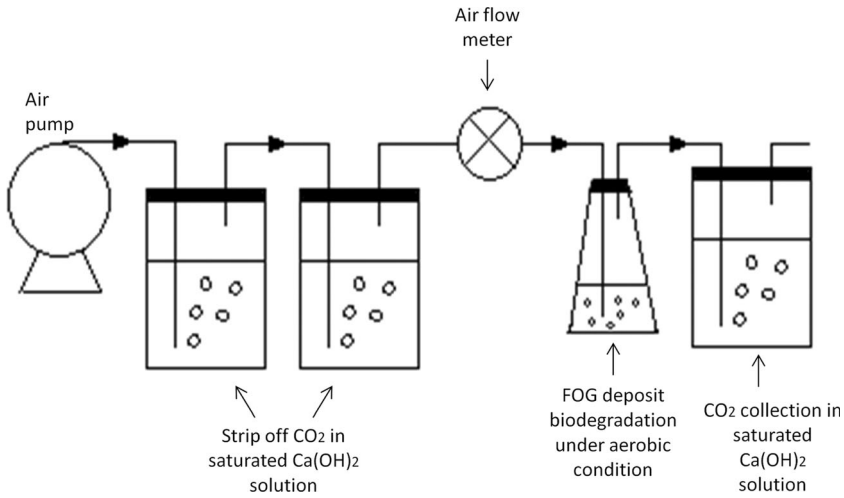

Fig. 1 Schematic plot of the experimetnal setup for the biodegradation of calcium palmitate under aerobic condition

collecting flask. The amount of $CaCO_3$ in the CO_2 collecting flask was measured as TSS according to *Standard Methods* (APHA 2012). Under anaerobic conditions, 6 ml of headspace gas sample was collected from each anaerobic test bottle using a gas sampling syringe with valve (Fisher Scientific) and then injected into a gas chromatograph (Agilent Technologies 6890N network GC system) fitted with two columns HP-Plot Q and HP-Plot 5A (Agilent Technologies) using a thermal conductivity detector (TCD) to quantify CO_2 and CH_4. Liquid samples were used for pH measurement and for anion quantification. For ion analysis, 1 ml of solution was collected using a 3-ml syringe (BD, NY) from each test bottle and then centrifuged at 10,000×*g* for 5 min. The supernatant was collected for nitrate and sulfate analysis using an ion chromatograph system (DIONEX ICS-1100).

Stoichiometric calculation

Stoichiometric equations for the biodegradation of palmitate under aerobic (Eq. 1), nitrate-reducing (Eq. 2), and sulfate-reducing (Eq. 3) conditions were developed. No equation under methanogenic condition was developed because of the lack of significant palmitate biodegradation under the methanogenic condition in this study. Bacterial biomass used the generic formula $C_5H_7O_2N$, and both the fractions of electron equivalent for cell synthesis (f_s) and energy (f_e) were assumed to be 50 %.

$$\frac{1}{4}O_2+\frac{2}{92}H^++\frac{2}{92}C_{16}H_{31}O_2^-+\frac{1}{20}HCO_3^- +\frac{1}{20}NH_4^+\rightarrow\frac{13.6}{92}CO_2+\frac{1}{20}C_5H_7O_2N+\frac{27.4}{92}H_2O \quad (1)$$

$$\frac{1}{5}NO_3^-+\frac{20.4}{92}H^++\frac{2}{92}C_{16}H_{31}O_2^-+\frac{1}{20}HCO_3^- +\frac{1}{20}NH_4^+\rightarrow\frac{13.6}{92}CO_2+\frac{1}{20}C_5H_7O_2N+\frac{36.6}{92}H_2O \quad (2)$$

$$\frac{1}{8}SO_4^{2-}+\frac{19.25}{92}H^++\frac{2}{92}C_{16}H_{31}O_2^-+\frac{1}{20}HCO_3^- +\frac{1}{20}NH_4^+\rightarrow\frac{13.6}{92}CO_2+\frac{1}{20}C_5H_7O_2N+\frac{1}{16}H_2S +\frac{1}{16}HS^-+\frac{27.4}{92}H_2O \quad (3)$$

LCFA profile analysis

At the end of microcosm experiment, LCFA profiles in all microcosms were determined using procedures previously described (Ichihara and Fukubayashi 2010). Briefly, remaining liquid and solid in the microcosms were completely mixed and then filtered through Whatman qualitative filter paper (pore size>11 μm). After drying at 105 °C overnight, 0.1 g solid on the filter paper was dissolved in 0.2 ml toluene in a screw-capped glass test tube, to which a 4-mg internal standard (tridecanoin, C13:0) was added. To this mixture, 1.50 ml of methanol and 0.30 ml of 8.0 % HCl solution in methanol were added sequentially and then incubated at 45 °C for 16 h. After cooling to room temperature, 1 ml of hexane and 1 ml of water were added and vortexed for 1 min to extract fatty acid methyl esters (FAMEs). After settlement for 10 min, the hexane layer was transferred to a new tube containing anhydrous sodium sulfate to remove residual water. Analysis for FAMEs was performed on a Hewlett Packard 5890 SERIES II Gas Chromatograph with a flame ionization detector (FID) using

split injection. A capillary RT-2560 column (Restek; Bellefonte, PA) was used, and the temperature gradient was 100 °C with a 4-min hold time, increased at 3 °C per min to a final temperature of 240 °C.

Analysis of active biomass

Active biomass concentration in microcosms was estimated based on protein content after cell lysis (More et al. 1994; Yucesoy et al. 2012). Briefly, 1 ml of sample from each microcosm was first centrifuged at 13,000×*g* for 5 min to pellet microbial biomass. After the supernatant was decanted, the cell pellet was resuspended in 0.375 ml phosphate buffer (0.1 M, pH=8) and then transferred to a 2-ml polypropylene microcentrifuge tube. Cell lysis was achieved by spiking 0.5 ml of the cell lysis solution (SDS-Tris-NaCl: 10 % SDS, 100 mM NaCl, 500 mM Tris (pH=8)), followed by bead beating with 0.2 g of acid-washed glass beads (300 μm diameter; Sigma-aldrich, MO) on a Vortex-genie 2 (Scientific industries, NY) at maximum speed for 10 min. Subsequently, the tube was centrifuged at 12,000×*g* for 3 min, and the supernatant was then used for protein analysis using Pierce BCA protein assay kit (Thermo Scientific, IL) following the manufacturer's procedure.

Microbial community analysis using Illumina sequencing

Microbial communities in the initial innoculum and select samples from the microcosm experiments were analyzed using Illumina sequencing of the 16S rRNA gene amplicons. For the microcosm experiments, 1 ml of liquid samples was collected from each microcosm on day 60 and day 95 after thorough mixing. Microbial biomass in the liquid samples were pelleted by centrifugation at 13,000×*g* for 5 min. Biomass pellets and the FOG deposit sample used as initial inoculum were subjected to DNA extraction using the PowerSoil DNA isolation kit (MO BIO) following the manufacturer's procedure.

Illumina sequencing was conducted at the DNA Services Facility at the University of Illinois at Chicago. Briefly, PCR amplification was conducted in triplicates for each sample using the primer set of 515f/806r to amplify the hypervariable V4 region of the 16S rRNA gene. Amplicons of the triplicate PCR reactions were pooled and then sequenced using an Illumina HiSeq 2000 instrument. De novo assemble of paired end reads was performed with the software package CLC Genomics Workbench Version 6.0 (CLC bio, Cambridge, MA), and the resulting FASTQ files were trimmed using a cutoff quality score of Q15 and read length of larger than 200 bp. The QIIME (1.7.0) software package was used to analyze Illumina sequence data following the procedure of Kuczynski et al. (Kuczynski et al. 2011). Operational taxonomic units (OTUs) were identified based on 97 % level sequence identity, and the relative abundance of individual OTUs were reported in the OTU table. The phylogenetic information of the OTUs was obtained by alignment with reference sequences in the Greengenes Database. Majority of the OTUs were assigned phylogeny at the genus level, while a small number of OTUs were resolved at the species level or at coarser levels (family, class). The sequence data used in this study have been submitted to GenBank and can be retrieved under the accession number SRP049485.

Results

Biodegradation of calcium palmitate under different redox conditions

Biodegradation of calcium palmitate, as indicated by CO_2 generation in the microcosms, was very slow and sensitive to redox conditions (Fig. 2). After 110 days of incubation, significant amounts of CO_2 were detected in the microcosms under aerobic or nitrate-reducing conditions. Only trace amounts of CO_2 were detected in microcosms under sulfate-reducing and methanogenic conditions (Fig. 2), indicating negligible biodegradation under those redox conditions. The CO_2 production rate under the aerobic condition (averaging 38 mg/l-day) was approximately 13 times higher than that under the nitrate-reducing condition (averaging 3 mg/l-day), indicating the biodegradation of calcium palmitate was most

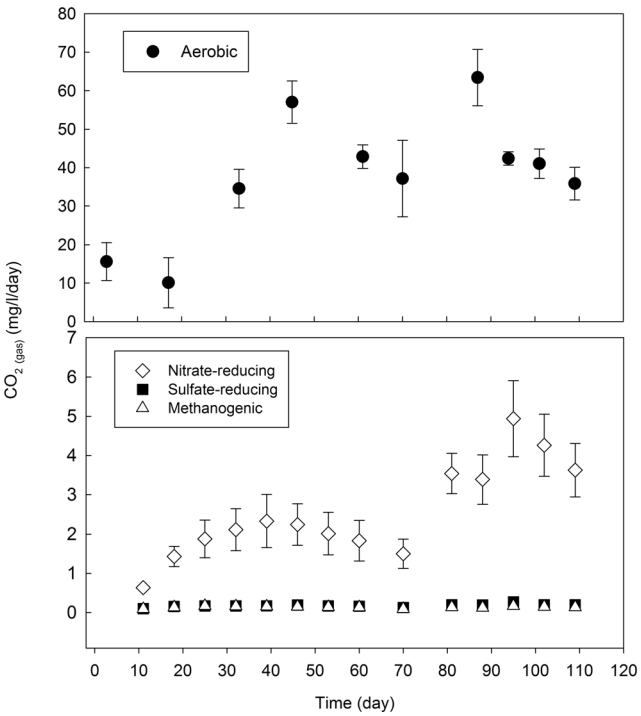

Fig. 2 CO_2 generation under aerobic condition, nitrate-reducing condition, sulfate-reducing condition, and methanogenic condition

efficient under aerobic condition. An average 0.02 mg/l-day CO_2 production rate was obtained in the autoclaved negative control based on measurements of CO_2 made on days 40, 80, and 110 (data not shown), which was negligible in comparison with the average CO_2 production rate under the sulfate-reducing condition (0.18 mg/l-day) and the methanogenic condition (0.14 mg/l-day).

The observed variation in biodegradation potentials was also supported by the consumption of sulfate and nitrate as electron acceptors under sulfate-reducing and nitrate-reducing conditions, respectively (Fig. 3), as well as the production of methane under the methanogenic condition (data not shown). The microcosms under nitrate-reducing conditions showed continuous decrease of nitrate concentration from 3720 to 1180 mg/l, while the sulfate-reducing microcosms showed significantly less decrease in sulfate, only from 3500 to 3205 mg/l, corroborating the observation made in Fig. 2. CH_4 was consistently below detection limit in the methanogenic microcosms (data not shown), which is in line with the very small amount of CO_2 generated under methanogenic condition (Fig. 2).

Based on the total amount of CO_2 generated during the 110 days, the mass percentage of calcium palmitate degradation under different redox conditions can be estimated using Eqs. 1–3. Under the aerobic condition, a total of 0.015 mol of CO_2 was produced, which corresponded to 0.0022 mol of palmitate according to Eq. 1 and accounted for 22 % of calcium palmitate introduced to the reactors. For nitrate-reducing condition, only 0.62 mmol of CO_2 was produced, indicating that merely 0.91 % of calcium palmitate was biodegraded according to Eq. 2. This is corroborated by the amount of nitrate consumption (0.82 mmol), which corresponded to a theoretical production of 0.61 mmol of CO_2, which is highly matched by the detected amount of CO_2 under the nitrate-reducing condition. Similarly, the detected consumption of 0.038 mmol of sulfate corresponded to a theoretical production of 0.045 mmol of CO_2 (Eq. 3), which is close to the detected amount of 0.043 mmol of CO_2, indicating that only 0.06 % of calcium palmitate was biodegraded under the sulfate-reducing condition. Thus, the percentage of calcium palmitate biodegradation under aerobic condition was 24 times and 363 times higher than that under nitrate-reducing condition and sulfate-reducing condition, respectively.

The addition of 200 mg/l Ca^{2+} at day 80 and day 88 led to significant increase of CO_2 generation in the nitrate-reducing microcosms (paired *t* test, $P=0.005$). However, the difference in CO_2 production was not significant in the aerobic microcosms (paired *t* test, $P=0.78$), sulfate-reducing microcosms (paired *t* test, $P=0.06$), and methanogenic microcosms (paired *t* test, $P=0.60$).

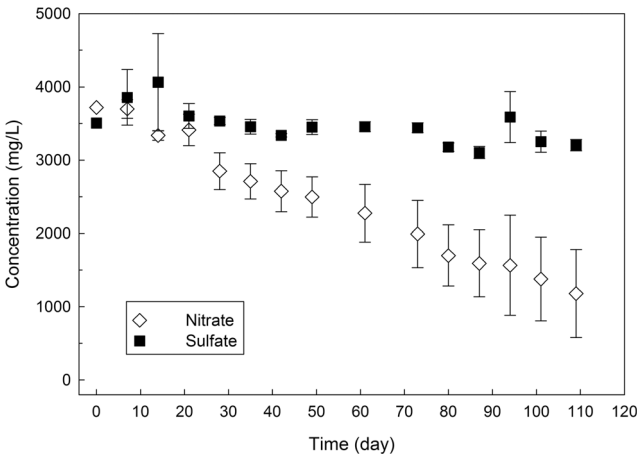

Fig. 3 The change of nitrate and sulfate under nitrate-reducing condition and sulfate-reducing condition, respectively

LCFA profiles under different redox conditions

A total of six LCFAs (C14:0, C15:0, C16:0, C16:1, C17:0, and C18:0) were detected, and their percentages were calculated for the microcosms under different redox conditions as well as the negative control (Fig. 4). C16:0 is the sole carbon substrate added to the microcosms, and C14:0 is considered to be the biodegradation product through β-oxidation. The LCFAs may also be derived from the lipid content of the bacterial biomass as bacteria lipids contain appreciable amount of C14 to C18 saturated and monounsaturated fatty acids (Ratledge and Wilkinson 1989). Compared to the anaerobic conditions and the negative control, the aerobic microcosms contained the lowest percentage of C16:0 (87.5 %) and

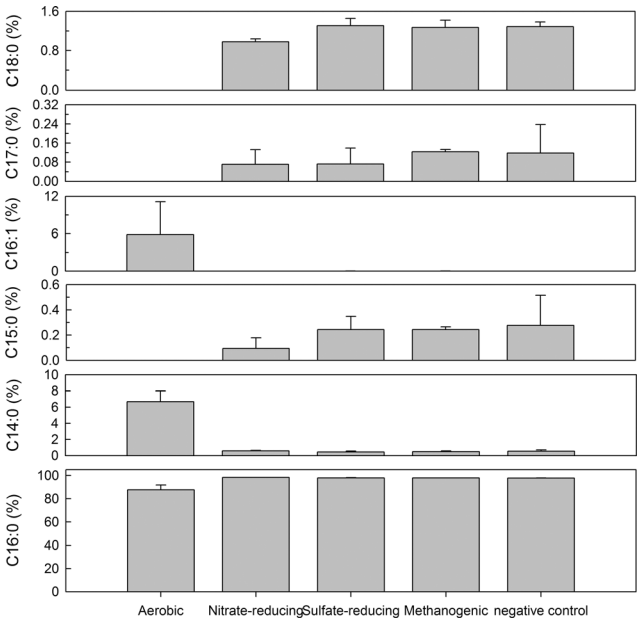

Fig. 4 LCFA profiles in all microcosms at the end of microcosm experiment

the highest percentage of C14:0 (6.7 %), supporting the highest efficiency of calcium palmitate biodegradation observed in the aerobic microcosms (Fig. 2). The microcosms under anaerobic conditions and negative control contained higher percentages of C16:0 (97.8–98.3 %) and very small percentages of C14:0 (0.5–0.6 %), which is consistent with the lower biodegradation potential of calcium palmitate observed under anaerobic conditions (Fig. 2). Among anaerobic conditions and negative control, no significant difference was found when comparing the percentage of C14 between each other (one-way ANOVA, P=0.51). Similarly, high similarity was found when comparing the percentage of C16 among the sulfate-reducing condition, the methanogenic condition, and the negative control (one-way ANOVA, P=0.50). However, the higher percentage of C16 was obtained under nitrate-reducing condition than other anaerobic conditions and the negative control (one-way ANOVA, P=0.01), which may be resulted from the production of bacterial biomass due to the biodegradation of calcium palmitate.

As for the fatty acids only derived from bacteria lipids such as C16:1, C15:0, C17:0, and C18:0, difference was also found among the different redox conditions and the negative control. C16:1 was only detected in the microcosms under aerobic condition, while C15:0, C17:0, and C18:0 were only observed under anaerobic conditions and the negative control. The lowest percentages of C15:0, C17:0, and C18:0 were obtained in the nitrate-reducing microcosms while the percentage of C17:0 was slightly (but not significantly) lower in the microcosms under sulfate-reducing condition (0.07 %) and that under the methanogenic condition (0.12 %). All these differences of fatty acids derived from bacteria lipids may be a result of different composition of microbial communities due to palmitate biodegradation under different redox conditions. No significant difference was obtained between the methanogenic condition and the negative control when comparing the percentages of C15 (t test, P=0.83), C17 (t test, P=0.94), and C18 (t test, P=0.90). The high similarity of fatty acid profiles between the methanogenic condition and the negative control corroborated the observation that calcium palmitate was not biodegraded in the microcosms under methanogenic condition.

Microbial biomass

Similar to the result of CO_2 production, the biodegradation of calcium palmitate led to a significant increase of microbial biomass in the aerobic microcosms and nitrate-reducing microcosms, while the sulfate-reducing and methanogenic microcosms showed no significant difference in microbial biomass (Fig. 5). The plateau of microbial biomass was reached after day 50 with the average concentration of 12.53 mg/l protein in the aerobic microcosms and 3.89 mg/l protein in the nitrate-reducing microcosms. These results supported the observation that calcium palmitate can be biodegraded more efficiently under aerobic condition than under nitrate-reducing condition. The highest concentration of microbial biomass observed at day 61 in the nitrate-reducing microcosms was considered as an outlier because the concentration was 11.1 mg/l that is outside the 1.5×IQR range (−3.0, 9.8), and the nitrate reduction rate was not increased significantly around day 60 (Fig. 3).

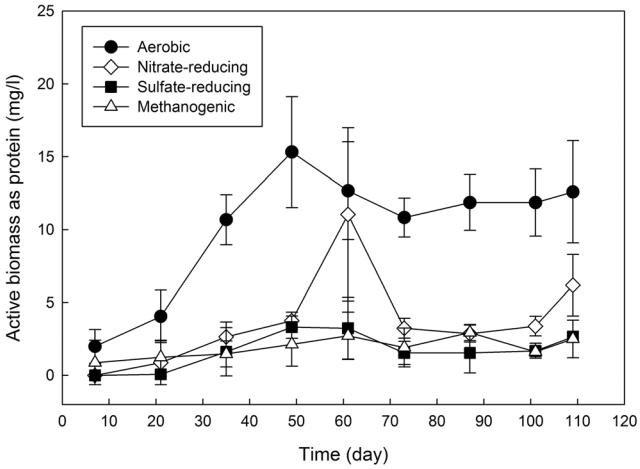

Fig. 5 The change of microbial biomass as protein under aerobic condition, nitrate-reducing condition, sulfate-reducing condition, and methanogenic condition

The addition of calcium did not lead to a significant change of microbial biomass in the aerobic microcosms (paired t test, P=0.64), nitrate-reducing microcosms (paired t test, P=0.61), sulfate-reducing microcosms (paired t test, P=0.51), and methanogenic microcosms (paired t test, P=0.88). Only a slight increase of microbial biomass at the end was observed in the microcosms under aerobic and nitrate redox conditions.

Microbial community composition

The microbial communities in all samples were determined using Illumina sequencing of 16S rRNA gene amplicons. Thirteen most abundant OTUs were detected in microbial community analysis, and the dominant OTUs were compared among different redox conditions to determine the similarity between microbial communities (Table 1). At the class level, 7 out of 13 OTUs were assigned to *Gammaproteobacteria*. Under the aerobic condition, significant changes of the composition of microbial community were observed. The most dominant OTU was first shifted from *Sphingobacteriia* (in inoculum) to *Arcobacter* within the *Epsilonproteobacteria* class (in A60) that was not detected in the inoculum, then to *Gammaproteobacteria* (in A95). The second dominant OTU in A60 belonged to *Flavobacteriia*, which only occupied 0.77 % in the inoculum. Another dominant OTU, which was not detected in the inoculum but observed in the aerobic microcosms, was *Acinetobacter* assigned to

Table 1 Heat map of 13 most abundant OTUs in microbial community samples

Class	Genus	Inoculum	A60	N60	A95	N95	S95	M95
Gammaproteobacteria		8.35	0.63	24.52	11.83	3.50	7.64	9.11
Sphingobacteriia		10.77	0.01	5.81	4.64	0.11	0.46	11.28
Thermoplasmata		9.41	0.00	2.56	3.58	0.00	0.00	5.48
Epsilonproteobacteria	*Arcobacter*	0.00	20.34	0.03	6.33	23.68	0.39	0.00
Flavobacteriia		0.77	16.08	0.51	4.11	6.48	2.53	0.36
Alphaproteobacteria		1.37	0.08	1.92	2.05	8.13	16.59	1.44
Gammaproteobacteria	*Vibrio*	0.15	0.07	0.41	0.26	5.75	16.10	0.07
Gammaproteobacteria		2.18	0.00	8.10	1.92	0.09	0.53	1.37
Bacteroidia	*Bacteroides*	0.08	8.86	0.31	2.08	4.59	0.02	0.02
Gammaproteobacteria	*Acinetobacter*	0.00	6.07	0.03	3.45	2.57	0.00	0.11
Gammaproteobacteria	*Alteromonas*	0.03	0.00	0.39	0.07	4.13	6.13	0.02
Gammaproteobacteria	*Marinomonas*	0.00	0.00	0.04	0.01	4.55	14.11	0.00
Gammaproteobacteria	*Pseudoalteromonas*	0.01	0.00	0.55	0.07	0.62	6.69	0.00

20-25% 15-20% 10-15% 5-10% 1-5% 0.5-1% 0.1-0.5% 0.01-0.1% 0.00-0.01%

Gammaproteobacteria. As more calcium palmitate was biodegraded, more OTUs became abundant from A60 to A95. Similarly, the composition of microbial community was significantly changed under nitrate-reducing condition from that in inoculum. The most dominant OTU was changed from *Sphingobacteriia* (in inoculum) to *Gammaproteobacteria* (in N60), then to *Arcobacter* affiliated with *Epsilonproteobacteria* (in N95). The dominant OTUs, which were not detected in inoculum but in N95, were *Arcobacter* affiliated with *Epsilonproteobacteria*, *Acinetobacter* assigned to *Gammaproteobacteria*, and *Marinomonas* assigned to *Gammaproteobacteria*. Although the samples A95 and N60 are from different redox conditions, they were dominated by the same OTU that belongs to the class *Gammaproteobacteria*. The dominant OTU for samples A60 and N95 was an *Arcobacter* within the *Epsilonproteobacteria* class. For sulfate-reducing condition, differences of the microbial community composition were also detected as the dominant OTU assigned with *Marinomonas* in S95 was not identified in the inoculum, and the dominant classes in S95 were *Alphaproteobacteria* and *Gammaproteobacteria*, which are different from the dominant classes in the inoculum. In contrast to above redox conditions, high similarity was found between inoculum and M95 as they were dominated by the same OTU assigned with *Sphingobacteriia* as well as the percentage of each abundant OTU was similar between each other. This result also supported the observation that calcium palmitate was not biodegraded in the microcosms under methanogenic condition.

Discussion

Theoretically, the LCFAs are metabolized to CO_2 via β-oxidation under aerobic, nitrate redox and sulfate redox conditions or to CH_4 by hydrogenotrophic and acetoclastic methanogens (Salam et al. 2012; Sousa et al. 2007). The observation of CO_2 generation and the increase of microbial biomass in the aerobic microcosms indicated that calcium palmitate can be biodegraded by aerobic microorganisms in the simulated sewer environment, which is consistent with the previous observation that many of the LCFAs are susceptible to degradation by aerobic microorganisms (Loehr and Roth 1968). However, calcium palmitate was not completely degraded within 110 days, which may be due to its low solubility as low solubility generally limits the biodegradation of 16 and 18 carbon saturated acids (Novak and Kraus 1973). The most efficient biodegradation of calcium palmitate was observed under aerobic condition, which follows the general energetic difference between aerobic and anaerobic processes (Thauer et al. 1977). Similar biodegradation trend was also observed in the study of crude oil biodegradation under different reducing conditions (Hasinger et al. 2012). As FOG deposits tend to form along pipe cross-sections above the low-flow water line (Keener et al. 2008), FOG deposits would be efficiently biodegraded on at the interface of FOG deposits and air in sewer lines.

As for nitrate-reducing condition, calcium palmitate was also biodegraded with lower biodegradation efficiency than the aerobic condition but with much higher biodegradation

potential than sulfate-reducing condition and methanogenic condition. Since layers of debris were observed to intersperse FOG deposits (Keener et al. 2008), food particles or detergents, which are the source of nitrate, was assumed to accumulate as debris inside FOG deposits. Thus, it is possible that the biodegradation of FOG deposits would occur inside FOG deposits under nitrate-reducing condition while the surface of FOG deposits would generally undergo aerobic biodegradation.

Although no significant generation of CO_2 and active biomass was observed in sulfate-reducing microcosms, the small reduction in sulfate suggested that calcium palmitate, the sole carbon and electron source, was biodegraded, albeit quite slowly in the sulfate-reducing microcosms. Another evidence to support the occurrence of calcium palmitate biodegradation under sulfate-reducing condition is the observation that microbial community S95 was different from inoculum as they were dominated by different OTUs. In addition, some of the dominant bacteria in S95, such as *Vibrio*, *Pseudoalteromonas*, and *Marinomonas*, have previously been identified as fuel oil-degrading species (Alonso-Gutierrez et al. 2008). The recalcitrance of calcium palmitate to biodegradation under sulfate-reducing condition is also confirmed by another study of crude oil biodegradation showing that low- to mid-weight carbon range (carbon numbers 11–25) is difficult to be biodegraded under sulfate-reducing condition (Hasinger et al. 2012).

Since the addition of calcium exhibited positive effect on biodegradation of LCFAs (Hatamoto et al. 2007; Roy et al. 1985) and calcium tends to accumulate on FOG deposits in sewer lines (He et al. 2011; Williams et al. 2012), it is possible that the accumulation of calcium on FOG deposits may enhance the efficiency of palmitate biodegradation in sewer lines. However, no significant difference was observed after the addition of calcium at days 80 and 88 in the aerobic microcosms, sulfate-reducing microcosms, and methanogenic microcosms. Only the CO_2 generation was significantly increased in the nitrate-reducing microcosms. Nevertheless, the nitrate reduction rate and microbial biomass were not significantly changed in this scenario. Therefore, it is possible that some CO_2 was released from HCO_3^- in solution to headspace in the nitrate-reducing microcosms as the pH dropped from 9.1 to 7.6 (data not shown) as a result of calcium addition. As it was hypothesized that the toxicity of palmitic acid was reversed by the precipitation of palmitic acid, the mole ratio of palmitic acid to calcium equal to 2 (1 mol of calcium can precipitate 2 mol of palmitic acid) is the threshold to determine the effect of calcium addition, and its positive effect on LCFA biodegradation was observed when the mole ratio of fatty acid to calcium was changed from greater than 2 to lower than 2 (Roy et al. 1985). In this study, it is very likely that the mole ratio was already lower than 2 before the addition of calcium. Thus, no positive effect of calcium addition on palmitate biodegradation was observed in all microcosms.

Significant difference was observed when comparing the composition of microbial community under different redox conditions, which corroborates the observation of different composition of fatty acids derived from bacteria lipids under different redox conditions. With the presence of microbial biomass, the consumption of C16:0 could not be determined based on the analysis of fatty acid profile. Nevertheless, the percentage of C16:0 rarely exceeds 50 % in microbial lipids (Bishop and Bermingham 1973; Suzuki and Komagata 1983). Thus, the high percentage of C16:0, which is greater than 85 % under all redox conditions, indicated that palmitate was not degraded completely under all redox conditions. This is also supported by the theoretical estimation of calcium palmitate biodegradation that, even under aerobic condition, 78.2 % of palmitate was not degraded.

Some fundamental insights into the efficient biodegradation of calcium palmitate were given by analyzing the microbial communities in the aerobic microcosms and nitrate-reducing microcosms. Microbial communities A95 and N60 were dominated by the same OTU assigned with *Gammaproteobacteria* that is commonly associated with substrates rich in organic carbon in aquatic environments (Fazi et al. 2005; Kirchman 2002; Simon et al. 2002). Many species in the class of *Gammaproteobacteria*, some of which are nitrate-reducing bacteria (Alain et al. 2012), have demonstrated capabilities in degrading hydrocarbons (Alonso-Gutierrez et al. 2008; Niepceron et al. 2013). The most dominant OTU in A60 and N95 was an *Arcobacter*, which was also dominant in an oil sand reservoir (Hubert et al. 2012). Another dominant OTU in A60 and N95 but not in inoculum was an *Acinetobacter*, which was used to degrade oil tank sludge (Matsui et al. 2014). High similarity between A95 and N60 as well as A60 and N95 suggested that some dominant populations, such as *Arcobacter* and *Acinetobacter*, may degrade calcium palmitate effectively under both aerobic and nitrate-reducing conditions.

To our best knowledge, this is the first report discussing the biodegradation of FOG deposits using model compound calcium palmitate under redox conditions relevant to sewer environment. Based on our data, calcium palmitate could be biodegraded under aerobic condition and very slowly under nitrate-reducing condition, indicating that the biodegradation of FOG deposits may be a factor in the accumulation of FOG deposits in sewer lines. Since some dominant populations in the aerobic and nitrate-reducing microcosms exhibited the capability to degrade calcium palmitate under aerobic condition or nitrate redox condition, further study on these populations and their functional genes could shed more light on this microbial process and eventually help develop engineering solutions for SSOs control in the future.

Acknowledgements We would like to thank the United States Environmental Protection Agency (USEPA grant: R834871) for funding this research. The contents of this research are solely the responsibility of the grantee and do not necessarily represent the official views of the USEPA. Further, USEPA does not endorse the purchase of any commercial products or services mentioned in the publication.

References

Alain K, Harder J, Widdel F, Zengler K (2012) Anaerobic utilization of toluene by marine *alpha*- and *gammaproteobacteria* reducing nitrate. Microbiol-Sgm 158:2946–2957. doi:10.1099/Mic. 0.061598-0

Alonso-Gutierrez J, Costa MM, Figueras A, Albaiges J, Vinas M, Solanas AM, Novoa B (2008) *Alcanivorax* strain detected among the cultured bacterial community from sediments affected by the 'Prestige' oil spill. Mar Ecol Prog Ser 362:25–36. doi:10.3354/Meps07431

Alves MM, Pereira MA, Sousa DZ, Cavaleiro AJ, Picavet M, Smidt H, Stams AJM (2009) Waste lipids to energy: how to optimize methane production from long-chain fatty acids (LCFA). Microbiol Biotechnol 2(5):538–550. doi:10.1111/j.1751-7915.2009.00100.×

APHA (2012) Standard methods for the examination of water and wastewater, 22nd edn. American Water Works Assn, Washington, DC

Becker P, Koster D, Popov MN, Markossian S, Antranikian G, Markl H (1999) The biodegradation of olive oil and the treatment of lipid-rich wool scouring wastewater under aerobic thermophilic conditions. Water Res 33(3):653–660

Bishop EA, Bermingham MAC (1973) Lipid composition of Gram-negative bacteria, sensitive and resistant to streptomycin. Antimicrob Agents Chemother 4(3):378–379

Canakci M (2007) The potential of restaurant waste lipids as biodiesel feedstocks. Bioresour Technol 98(1):183–190. doi:10.1016/j.biortech.2005.11.022

Fazi S, Amalfitano S, Pernthaler J, Puddu A (2005) Bacterial communities associated with benthic organic matter in headwater stream microhabitats. Environ Microbiol 7(10):1633–1640. doi:10.1111/j.1462-2920.2005.00857.×

Hasinger M, Scherr KE, Lundaa T, Brauer L, Zach C, Loibner AP (2012) Changes in iso- and n-alkane distribution during biodegradation of crude oil under nitrate and sulphate reducing conditions. J Biotechnol 157(4):490–498. doi:10.1016/j.jbiotec.2011.09.027

Hatamoto M, Imachi H, Yashiro Y, Ohashi A, Harada H (2007) Diversity of anaerobic microorganisms involved in long-chain fatty acid degradation in methanogenic sludges as revealed by RNA-based stable isotope probing. Appl Environ Microbiol 73(13):4119–4127. doi:10.1128/Aem. 00362-07

He Z, Minteer SD, Angenent LT (2005) Electricity generation from artificial wastewater using an upflow microbial fuel cell. Environ Sci Technol 39(14):5262–5267. doi:10.1021/Es0502876

He X, Iasmin M, Dean LO, Lappi SE, Ducoste JJ, de los Reyes FL (2011) Evidence for fat, oil, and grease (FOG) deposit formation mechanisms in sewer lines. Environ Sci Technol 45(10):4385–4391. doi:10.1021/Es2001997

He X, de los Reyes FL, Leming ML, Dean LO, Lappi SE, Ducoste JJ (2013) Mechanisms of fat, oil and grease (FOG) deposit formation in sewer lines. Water Res 47(13):4451–4459. doi:10.1016/j.watres.2013.05.002

Hubert CRJ, Oldenburg TBP, Fustic M, Gray ND, Larter SR, Penn K, Rowan AK, Seshadri R, Sherry A, Swainsbury R, Voordouw G, Voordouw JK, Head IM (2012) Massive dominance of *Epsilonproteobacteria* in formation waters from a Canadian oil sands reservoir containing severely biodegraded oil. Environ Microbiol 14(2):387–404. doi:10.1111/j.1462-2920.2011.02521.×

Ichihara K, Fukubayashi Y (2010) Preparation of fatty acid methyl esters for gas-liquid chromatography. J Lipid Res 51(3):635–640. doi:10.1194/Jlr.D001065

Keener KM, Ducoste JJ, Holt LM (2008) Properties influencing fat, oil, and grease deposit formation. Water Environ Res 80(12):2241–2246. doi:10.2175/193864708×267441

Kirchman DL (2002) The ecology of *Cytophaga-Flavobacteria* in aquatic environments. FEMS Microbiol Ecol 39(2):91–100. doi:10.1111/J.1574-6941.2002.Tb00910.×

Kuczynski J, Stombaugh J, Walters WA, Gonzalez A, Caporaso JG, Knight R (2011) Using QIIME to analyze 16S rRNA gene sequences from microbial communities. Current protocols in bioinformatics / editoral board, Andreas D Baxevanis [et al.] Chapter 10: Unit 10 7 doi:10.1002/0471250953.bi1007s36

Lalman JA, Bagley DM (2000) Anaerobic degradation and inhibitory effects of linoleic acid. Water Res 34(17):4220–4228. doi:10.1016/S0043-1354(00)00180-9

Lalman JA, Bagley DM (2001) Anaerobic degradation and methanogenic inhibitory effects of oleic and stearic acids. Water Res 35(12):2975–2983. doi:10.1016/S0043-1354(00)00593-5

Lee KH, Park KY, Khanal SK, Lee JW (2013) Effects of household detergent on anaerobic fermentation of kitchen wastewater from food waste disposer. J Hazard Mater 244:39–45. doi:10.1016/j.jhazmat.2012.10.073

Li YY, Sasaki H, Yamashita K, Seki K, Kamigochi I (2002) High-rate methane fermentation of lipid-rich food wastes by a high-solids co-digestion process. Water Sci Technol 45(12):143–150

Li ZK, Wrenn BA, Venosa AD (2005) Anaerobic biodegradation of vegetable oil and its metabolic intermediates in oil-enriched freshwater sediments. Biodegradation 16(4):341–352. doi:10.1007/s10532-004-2057-6

Loehr RC, Roth JC (1968) Aerobic degradation of long-chain fatty acid salts. J - Water Pollut Control Fed 40(11):385–403

Matsui T, Yamamoto T, Shinzato N, Mitsuta T, Nakano K, Namihira T (2014) Degradation of oil tank sludge using long-chain alkane-degrading bacteria. Ann Microbiol 64(1):391–395. doi:10.1007/s13213-013-0643-8

More MI, Herrick JB, Silva MC, Ghiorse WC, Madsen EL (1994) Quantitative cell-lysis of indigenous microorganisms and rapid extraction of microbial DNA from sediment. Appl Environ Microbiol 60(5):1572–1580

Niepceron M, Martin-Laurent F, Crampon M, Portet-Koltalo F, Akpa-Vinceslas M, Legras M, Bru D, Bureau F, Bodilis J (2013) *GammaProteobacteria* as a potential bioindicator of a multiple contamination by polycyclic aromatic hydrocarbons (PAHs) in agricultural soils. Environ Pollut 180:199–205. doi:10.1016/j.envpol.2013.05.040

Novak JT, Kraus DL (1973) Degradation of long chain fatty acids by activated sludge. Water Res 7(6):843–851. doi:10.1016/0043-1354(73)90100-0

Pagaling E, Yang K, Yan T (2014) Pyrosequencing reveals correlations between extremely acidophilic bacterial communities with hydrogen sulphide concentrations, pH and inert polymer coatings at concrete sewer crown surfaces. J Appl Microbiol 117(1):50–64. doi:10.1111/Jam.12491

Pereira MA, Pires OC, Mota M, Alves MM (2005) Anaerobic biodegradation of oleic and palmitic acids: evidence of mass transfer limitations caused by long chain fatty acid accumulation onto the anaerobic sludge. Biotechnol Bioeng 92(1):15–23

Ratledge C, Wilkinson SG (1989) Microbial lipids, volume 2. Academic, London

Roy F, Albagnac G, Samain E (1985) Influence of calcium addition on growth of highly purified syntrophic cultures degrading long-chain fatty acids. Appl Environ Microbiol 49(3):702–705

Salam DA, Naik N, Suidan MT, Venosa AD (2012) Assessment of aquatic toxicity and oxygen depletion during aerobic biodegradation of vegetable oil: effect of oil loading and mixing regime. Environ Sci Technol 46(4):2352–2359. doi:10.1021/Es2037993

Shin HS, Kim SH, Lee CY, Nam SY (2003) Inhibitory effects of long-chain fatty acids on VFA degradation and beta-oxidation. Water Sci Technol 47(10):139–146

Simon M, Grossart HP, Schweitzer B, Ploug H (2002) Microbial ecology of organic aggregates in aquatic ecosystems. Aquat Microb Ecol 28(2):175–211. doi:10.3354/Ame028175

Sousa DZ, Pereira MA, Stams AJM, Alves MM, Smidt H (2007) Microbial communities involved in anaerobic degradation of unsaturated or saturated long-chain fatty acids. Appl Environ Microbiol 73(4):1054–1064. doi:10.1128/Aem. 01723-06

Suzuki K, Komagata K (1983) Taxonomic significance of cellular fatty acid composition in some coryneform bacteria. Int J Syst Bacteriol 33(2):188–200

Thauer RK, Jungermann K, Decker K (1977) Energy conservation in chemotrophic anaerobic bacteria. Bacteriol Rev 41(1):100–180

USEPA (2004) Report to Congress: Impacts and control of CSOs and SSOs. Office of Water, United States Environmental Protection Agency, Washington D.C. EPA B33-R-04-001

Williams JB, Clarkson C, Mant C, Drinkwater A, May E (2012) Fat, oil and grease deposits in sewers: characterisation of deposits and formation mechanisms. Water Res 46(19):6319–6328

Yucesoy E, Ludemann N, Lucas H, Tan J, Denecke M (2012) Protein analysis as a measure of active biomass in activated sludge. Water Sci Technol 65(8):1483–1489. doi:10.2166/Wst.2012.029